Mat. Res. Soc. Symp. Proc. Vol. 728 © 2002 Materials Research Society

Plasmon Scanned Surface-Enhanced Raman Scattering Excitation Profiles

Christy L. Haynes and Richard P. Van Duyne
Department of Chemistry, Northwestern University,
Evanston, Illinois 60208-3113, USA

ABSTRACT

Since the discovery of surface-enhanced Raman spectroscopy (SERS) in 1977, scientists have come to understand the enhancement mechanism, but have been unable to consistently optimize the weak signals inherent in Raman experiments. Surface-enhanced Raman signals originate from excitation of the localized surface plasmon resonance (LSPR) of a nanostructured metal surface, thus producing concentrated electromagnetic fields at the surface of the nanostructure. Design of the nanostructured metal substrate plays an important role in understanding and optimizing SERS experiments. In this research, the size-dependent optical properties accessible by nanosphere lithography (NSL) are exploited to fabricate topographically predictable SERS-active substrates with systematically varying LSPRs. Correlated micro-extinction and micro-Raman measurements, as well as quantitative implementation of a Raman standard, allow significant improvements over the current method used to optimize SERS experiments. The knowledge gained in the novel plasmon scanned SERS excitation profiles clearly indicates the substrate parameters necessary for experimental optimization and promotes further understanding of the SERS enhancement mechanism.

INTRODUCTION

The current widespread interest in size-dependent optical properties of nanomaterials is a consequence of their many applications in the fields of bio/chemosensors [1,2], optical devices [3], and surface-enhanced spectroscopies [4]. The signature optical property of a metallic nanoparticle is the localized surface plasmon resonance (LSPR). This resonance occurs when the correct wavelength of light strikes a metallic nanoparticle, causing the plasma of conduction electrons to oscillate collectively. The term LSPR is used because this collective oscillation is localized within the near surface region of the nanoparticle. The two consequences of exciting the LSPR are: 1) selective photon absorption and 2) generation of locally enhanced or amplified electromagnetic fields at the nanoparticle surface. The LSPR for noble metal nanoparticles in the 20 - few hundred nanometer size regime occurs in the visible and IR regions of the spectrum and can be measured by UV-visible-IR extinction spectroscopy. Because the material, size, shape, and dielectric environment dictate the characteristics of the LSPR [5], these properties also control the surface-enhancing capability of the nanostructured substrate.

The surface-enhanced analogs of spectroscopic techniques (i.e., surface-enhanced fluorescence, surface enhanced infrared absorption, and surface-enhanced second harmonic generation) are powerful because the spectroscopic signals are significantly larger than the unenhanced spectroscopy. For example, Raman scattering is an inherently weak process because only one out of every 10^8 photons scatters inelastically, but the discovery of surface-enhanced Raman scattering (SERS) allows the application of this sensitive and selective technique to many pressing experimental studies. Though the enhancement mechanism for ensemble-averaged

SERS (signal enhancement $\geq 10^6$) is well understood, the enhancement mechanism of single molecule SERS (signal enhancement $> 10^{14}$) is being hotly debated.

In general, the enhancement factor (EF) is greatly affected by differing surface roughness characteristics, and this variation can be investigated by performing surface-enhanced Raman excitation spectroscopy (SERES). Surprisingly, in the 25 years since the discovery of SERS, there has never been a detailed comparison of the LSPR spectra of regularly nanostructured surfaces and the SERES even though they are intimately linked through the electromagnetic (EM) enhancement mechanism. More than 4000 papers depicting SER spectra have been published, and yet there are less than 30 that address SERES. This is likely the result of the difficulty of SERES experiments and its typically low data point density. Wavelength scanned excitation profiling (WSEP) involves the measurement of SER spectra from a single substrate with many laser excitation wavelengths (λ_{ex}) [6]. WSEPs are plots of Raman intensity for a particular scattered wavelength (λ_{vib}) versus λ_{ex} that report the optimized λ_{ex} for that specific substrate and adsorbate. The inherent difficulty in WSEP lies in the fact that the number of data points is limited by the number of available λ_{ex}. Herein, we present a new method, called plasmon scanned excitation profiling (PSEP), to probe SERES by correlating spatially-resolved LSPR and SER spectra on nanolithographically fabricated Ag nanoparticles.

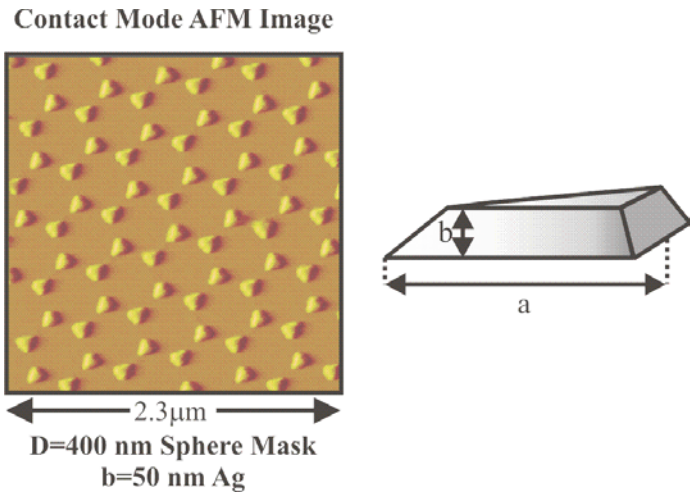

Figure 1. An AFM image of a standard NSL nanoparticle array and the geometry of a single nanoparticle.

The PSEP method capitalizes on the LSPR tunablility accessible with the nanosphere lithography (NSL) fabrication technique. Briefly, a colloidal crystal monolayer of size-monodisperse nanospheres is grown on a flat substrate of choice, and then the desired nanoparticle material is thermally evaporated through the nanosphere mask. Upon removing the nanospheres from the surface, homogeneous arrays of truncated tetrahedral nanoparticles with p6mm symmetry remain on the substrate (Figure 1). The aspect ratio of these electromagnetically uncoupled nanoparticles is easily tuned by varying nanosphere diameter and deposition thickness. Previous work has shown that the LSPR is tunable throughout visible and infrared wavelengths using the NSL technique [7].

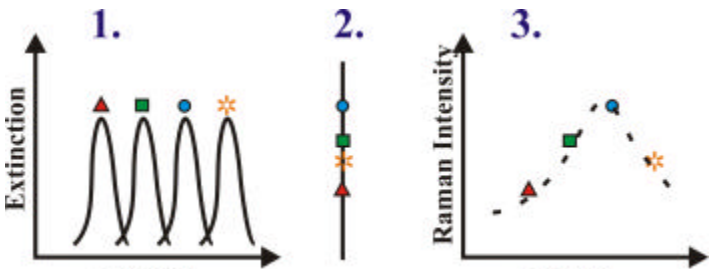

Figure 2. Schematic depiction of the PSEP process: 1) collect LSPR spectrum from dosed nanoparticle surface; 2) collect Raman spectrum from same area; and 3) plot the LSPR λ_{max} versus the Raman intensity of a chosen vibrational band.

In the PSEP experiment, both the LSPR and SERS measurements are spatially resolved and correlated. By interchanging a white light source with UV-vis detection and a laser light source with Raman detection, it is possible to

measure the LSPR and SER spectra from the same location on each sample. PSEPs are plots of the SERS enhancement factor for a particular λ_{vib} versus the LSPR maximum (λ_{max}). See the schematic in Figure 2.

EXPERIMENTAL DETAILS

Materials

Ag (99.99%, 0.50 mm diameter) was purchased from D. F. Goldsmith (Evanston, IL). Borosilicate glass substrates were Fisher brand No. 2 cover slips from Fisher Scientific (Pittsburgh, PA). Tungsten vapor deposition boats were acquired from R. D. Mathis (Long Beach, CA). Polystyrene nanospheres of various diameters (280 nm, 310 nm, and 400 nm in this work) were purchased from Interfacial Dynamics Corporation (Portland, OR). For all steps of substrate preparation, water purified with cartridges from Millipore (Marlborough, MA) to a resistivity of 18 M was used.

Nanoparticle surface preparation

Glass substrates were cleaned by immersion in 3:1 concentrated H_2SO_4:30% H_2O_2 at 80°C for one hour. After cooling, the substrates were rinsed repeatedly with water and then sonicated for 60 minutes in 5:1:1 H_2O:NH_4OH:30%H_2O_2 solution. Following sonication, the substrates were again rinsed repeatedly with water and then used immediately or stored in water for no longer than one week. Single layer periodic particle arrays were prepared using the NSL technique. Nanospheres used to form deposition masks on glass substrates were used as received without any further dilution with a surfactant solution. Once the 2D colloidal crystal deposition mask was formed, the substrates were mounted into the chamber of a modified Consolidated Vacuum Corporation (Rochester, NY) vapor deposition system. Ag films of varying thickness were then deposited over the nanosphere mask. The mass thickness for each film was measured using a Leybold Inficon XTM/2 deposition monitor quartz crystal microbalance (East Syracuse, NY). After the Ag deposition, the nanosphere mask was removed by sonicating the entire substrate in absolute ethanol for 3 minutes.

AFM characterization

AFM images were collected under ambient conditions using a Digital Instruments (Santa Barbara, CA) Nanoscope III microscope operating in either contact mode or intermittent contact mode. Etched Si nanoprobe tips with spring constants of approximately 0.15

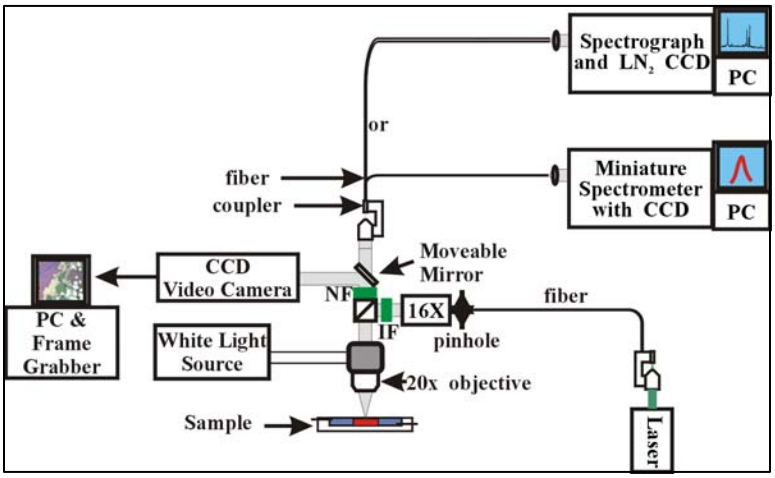

Figure 3. Instrument used to perform correlated micro-extinction and micro-Raman measurements for the PSEP process.

N m^{-1} were used. These conical shaped tips had a cone angle of 20° and an effective radius of curvature of 10 nm. The resonance frequency of the intermittent contact mode cantilevers was measured to be between 280-330 Hz. The AFM images presented here represent raw, unfiltered data.

Experimental apparatus

Figure 3 shows an instrument diagram. The probe lasers used include the 532.0 nm output of a Spectra-Physics (Mountain View, CA) Millennia Vs laser and the 632.8 nm output of a Coherent (Palo Alto, CA) Model 590 tunable dye laser. In each case, the laser light was fiber optically coupled into a modified Optiphot confocal microscope, the laser spot size was increased using a 16x beam expanding telescope, and interference filters (Omega Optical, Brattleboro, VT) were used to select the desired excitation wavelength. The dosed substrates were illuminated and the scattered light was collected with a 20x objective in standard back-scattering geometry. The scattered light passed through a holographic notch filter (Kaiser Optical Systems, Ann Arbor, MI) that eliminates the reflected laser light and the Rayleigh scattered light. The remainder of the light was focused with a 10x objective into a 200 μm core diameter multi-mode optical fiber (Ensign-Bickford, Simsbury, CT) that guides the light to the spectrometer. Light exiting this fiber was collimated with a home-built 4x beam expanding telescope. The collimated light was then focused onto the entrance slit (150 μm) of a single grating 0.5 meter Acton (Acton, MA) VM-505 monochromator and measured with a LN_2-cooled Roper Scientific (Trenton, NJ) Spec-10:400B CCD detector. In order to collect extinction spectra from the same area sampled with Raman spectroscopy, the microscope lamp was used as an excitation source (laser blocked) and the output fiber was directed to an Ocean Optics (Dunedin, FL) SD2000 spectrograph.

RESULTS AND DISCUSSION

Figure 4 shows the PSEPs for the ν_{8a} mode of benzenethiol adsorbed to NSL-fabricated surfaces with deposition thicknesses between 20 and 60 nm. All of the other vibrational modes of benzenethiol behave similarly. These PSEPs clearly show that the maximum SERS enhancement factors occur when the LSPR λ_{max} lies between λ_{ex} and λ_{vib}. Furthermore, both PSEPs exhibit two regimes of enhancement behavior. The majority of the sampled areas follow the average LSPR behavior, resulting in enhancement factors largely between 1 x 10^7 and 4 x 10^7 for LSPR λ_{max} values within a 160 nm window. However, a few sampled areas within a narrow LSPR λ_{max} range contribute larger than anticipated enhancement factors, i.e., 4 x 10^7 to 9 x 10^7.

The instrument used to perform PSEPs is shown in Figure 3. Using the known spot size of the 20x microscope objective (w = 4 μm), we determined the

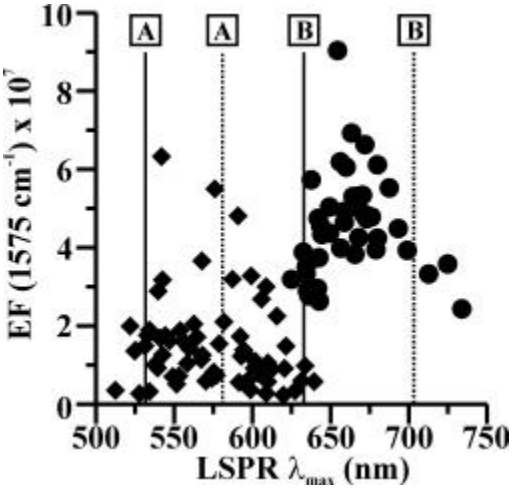

Figure 4. PSEP for the 1575 cm-1 band of benzenethiol with two different excitation wavelengths (λ_{ex}): (A) 532.0 nm and (B) 632.8 nm. For each λ_{ex}, both the wavelength location of the excitation (solid line) and the scattering (dashed line) are marked.

number of nanoparticles in the given spot size based on the nanoparticle areal density (7.2 % for single layer NSL-derived nanoparticles). At this point, we assume that the sampled area is perfectly covered in only single layer nanoparticles. Next, we calculate the exposed surface area of each nanoparticle based on its perpendicular bisector, a, and mass thickness, d_m. Assuming that each nanoparticle is a truncated tetrahedron, the exposed surface area is:

$$SA_{exposed} = \sqrt{3}d_m(2a - d_m) + \frac{\sqrt{3}(a - d_m)^2}{3} \quad (1)$$

We then use the largest measured packing density for benzenethiol molecules on the nanoparticle surface, 6.8×10^{14} molecules/cm^2 [8]. (Note: Different benzenethiol packing densities have been reported in the literature [9].) Any disorder in the self-assembled monolayer would contribute to a larger overall enhancement factor. Using this number of molecules per nanoparticle and the calculated number of nanoparticles in the probe area, we determine how many molecules are contributing to the measured SER signal on each sample (N_{surf}).

Neat, liquid benzenethiol in a thin glass cell was used as the Raman intensity standard. The probe volume of our confocal microscope with the 20x objective was found to be 7.5 pL (based on $1/e^2$ analysis). Using the density of benzenethiol, $\rho = 1.073$ g/mL, we determine that there are 4.399×10^{13} benzenethiol molecules contributing to the normal Raman signal measured from the standard (N_{vol}) at the beginning and end of each experiment.

SERS enhancement factors were calculated using the following equation [10]:

$$EF(1575\ \text{cm}^{-1}) = \frac{N_{vol} I_{surf}}{N_{surf} I_{vol}} \quad (2)$$

where I_{vol} and I_{surf} are the measured intensities, in analog/digital converter units per second per milliwatt, of a Raman/SER spectral peak from the standard and sample. Additionally, because we know that each probed area is not perfect (i.e., there were defects in the colloidal crystal mask), we account for imperfections by linearly correcting the enhancement factor based on the amplitude of the extinction spectrum. This gives us the final enhancement factor that is plotted versus LSPR λ_{max} to generate the PSEP.

The first regime of EF behavior is expected, but there are currently no theoretical studies that predict the second regime of behavior. We postulate that especially large EM fields are generated at "hot spots" on the nanoparticle surface when the geometric conditions for supporting a multipolar resonance are fulfilled. Multipole resonances are known to be very narrow [11], and may account for the narrow range of LSPR λ_{max} values contributing especially large enhancement factors. The large, highly homogeneous domains of NSL-fabricated nanoparticles generate probe areas with uniform LSPRs and electromagnetic field spatial profiles, making this effect obvious for the first time.

CONCLUSIONS

Data presented herein probes the correlated extinction and SERS spectra of benzenethiol adsorbed to NSL-fabricated silver substrates. The plasmon scanned excitation profile plots of LSPR λ_{max} versus the SERS intensity of any vibrational band demonstrate that SERS

experiments are optimized when the LSPR λ_{max} lies between the excitation wavelength and the scattering wavelength. Enhancement factors as large as 9×10^7 are measured from the optimized SERS substrate. In this investigation, exploitation of substrate design is used in an innovative new method to probe the SERS excitation profile; this method is simple to implement experimentally and provides both practical and fundamental insights into SERS experiments.

ACKNOWLEDGMENTS

The authors acknowledge support from the National Science Foundation (EEC-0118025 and DMR-0076097), the Army Research Office MURI program (DAAG-55-97-0133), and an ACS Division of Analytical Chemistry fellowship sponsored by GlaxoSmithKline (C.L.H.). We thank Prof. G. C. Schatz for many helpful conversations.

REFERENCES

1. J. J. Storhoff, R. Elghanian, R.C. Mucic, C. A. Mirkin, R. L. Letsinger, *J. Am. Chem. Soc.* **120**, 1959 (1998).
2. G. Pan, R. Kesavamoorthy, S. A. Asher, *J. Am. Chem. Soc.* **120**, 6525 (1998).
3. S. Asher, S.-Y. Chang, A. Tse, L. Liu, G. Pan, Z. Wu, P. Li, *Mater. Res. Soc. Symp. Proc.* **374**, 305 (1995).
4. S. Zou, C. T. Williams, E. K.-Y. Chen, M. J. Weaver, *J. Am. Chem. Soc.* **120**, 3811 (1998).
5. C. L. Haynes and R. P. Van Duyne, *J. Phys. Chem. B* **105**, 5599 (2001).
6. P. F. Liao, J. G. Bergman, D. S. Chemla, A. Wokaun, J. Melngailis, A. M. Hawryluk, N. P. Economou, *Chem. Phys. Lett.* **81**, 355 (1981).
7. T. R. Jensen, M. Duval Malinsky, C. L. Haynes, R. P. Van Duyne, *J. Phys. Chem. B.* **104**, 10549 (2000).
8. L.-J. Wan, M. Terashima, H. Noda, M. Osawa, *J. Phys. Chem. B* **104**, 3563 (2000).
9. C. M. Whelan, M. R. Smyth, C. J. Barnes, *Langmuir* **15**, 116 (1999).
10. R. P. Van Duyne, in *Chemical and Biochemical Applications of Lasers*, edited by C. B. Moore (Academic Press: New York, 1979) Volume 4, pp. 101-184.
11. K. L. Kelly, T. R. Jensen, A. A. Lazarides, G. C. Schatz, in *Metal Nanoparticles: Synthesis, Characterization, and Applications*, edited by D. Feldheim and C. Foss (Marcel-Dekker: New York, 2001) pp. 89-118.